



Published in final edited form as:

*Hypertension*. 2014 December ; 64(6): 1306–1313. doi:10.1161/HYPERTENSIONAHA.114.03775.

## A novel high-throughput in vitro model for identifying hemodynamic-induced inflammatory mediators of cerebral aneurysm formation

Kamil W. Nowicki, B.S.<sup>1</sup>, Koji Hosaka, Ph.D.<sup>1</sup>, Yong He, Ph.D.<sup>2</sup>, Peter S. McFetridge, Ph.D.<sup>3</sup>, Edward W. Scott, Ph.D.<sup>4</sup>, and Brian L. Hoh, M.D.<sup>1</sup>

<sup>1</sup>Department of Neurosurgery, University of Florida

<sup>2</sup>Department of Surgery, University of Florida

<sup>3</sup>Department of Biomedical Engineering, University of Florida

<sup>4</sup>Department of Molecular Genetics and Microbiology, University of Florida

### Abstract

Cerebral aneurysms are thought to develop at locations of hemodynamic shear stress, via an inflammatory process. The molecular mechanism that links shear stress to inflammation, however, is not completely understood. *Progress in studying this disease is limited by a lack of a suitable in vitro model.* To address this, we designed novel in vitro parallel-plate flow chamber models of a straight artery, a bifurcation, and a bifurcation aneurysm. We compared endothelial cell phenotypes across the three different models, and among microenvironments within each flow model, by cytokine array, ELISA and relative immunofluorescence. Human aneurysms express IL-8 and CXCL1, whereas normal arteries do not. The bifurcation aneurysm model showed significantly higher IL-8 and CXCL1 levels than both the straight artery and bifurcation models. *Within* the bifurcation and bifurcation aneurysm models, endothelial cells near the bifurcation or within the aneurysm sac microenvironments have significantly higher expression of CXCL1, and IL-8 and CXCL1, respectively, than at the straight proximal segment or the limbs of the bifurcation. Murine aneurysms express CXCL1, and it is the primary ELR+ CXC chemokine expressed, whereas normal arteries do not. CXCL1 antibody blockade results in significantly fewer murine aneurysms (13.3 vs 66.7%,  $p=0.0078$ ), decreased neutrophil infiltration and VCAM-1 expression than an IgG control. We successfully designed and validated a novel hemodynamic model of cerebral aneurysms *in vitro*. We also show that shear stress-induced CXCL1 plays a critical role in cerebral aneurysm formation.

### Keywords

aneurysm; hemodynamics; endothelial shear stress; endothelium; inflammation

---

Corresponding Author: Brian L. Hoh, M.D., PO Box 100265, Gainesville, FL 32610, Fax: 352-392-8413, Phone: 352-273-9000, brian.hoh@neurosurgery.ufl.edu.

Disclosures: None.

## Introduction

Cerebral aneurysms are focal dilations of cerebral arteries that can rupture and result in subarachnoid hemorrhage, leading to significant mortality and morbidity.<sup>1</sup> Computational flow dynamic (CFD) studies have implicated high wall shear stress (WSS) and wall shear stress gradients (WSSG) in initiating aneurysm development.<sup>2-5</sup> Hemodynamic shear stress has been implicated in activation of the inflammatory pathway through nuclear factor-kappa beta (NF- $\kappa$ β) in the endothelium.<sup>6</sup> Because animal studies are costly, time-consuming, and difficult to manipulate, an effective *in vitro* screening tool is needed in order to study the cell phenotypes and inflammatory mediators that occur in the context of cerebral aneurysm hemodynamic conditions.

To address this need, we designed novel *in vitro* parallel-plate flow chamber models of a straight artery, a bifurcation artery, and a bifurcation aneurysm, characterized by reproducible hemodynamic conditions in order to study the effect of shear stress on endothelial cell (EC) phenotypes at different microenvironment locations. Importantly, the model is simple, effective, and high throughput in that it is low-cost and only takes 24-48 hours to produce results. We propose that low shear stress and shear stress gradients at bifurcations and bifurcation aneurysms induce endothelial expression of specific inflammatory factors that promote aneurysm formation and growth.

## Methods

Detailed descriptions of all methods are available in the expanded methods section of the online data supplement.

### Parallel-Plate Flow Chamber Design

Uzarski et al. originally designed the parallel-plate chamber for a straight artery.<sup>7</sup> The idealized three flow models of a straight artery, bifurcation and bifurcation aneurysm were created based on previously published CFD studies<sup>3-5, 8</sup> and the anatomical dimensions of human cerebral arteries<sup>9</sup>.

### Modeling Shear Stress

Mesh generation was performed in Gambit 2.0 (ANSYS, Canonsburg, PA). CFD simulation using measured flow rates (Figure S1) was done in ANSYS Fluent (ANSYS, Canonsburg, PA). Post-processing and visualization of velocity streamlines, wall shear stress (WSS), and wall shear-stress gradient (WSSG) were performed in Tecplot 360 (Tecplot, Bellevue, WA).

### Shear Stress Experiments

Human umbilical vein endothelial cells (HUVECs) at passage 2-5 and pooled from 3 donors (Figure S2) were seeded on coverslips cut from tissue culture plastic dishes (Techno Plastic Products, Trasadingen, Switzerland) at a density of 20,000 cells/cm<sup>2</sup> and grown to confluence. ECs were exposed to pulsatile shear stress over 27 hours, and ultimately exposed to shear stress at 10-dyne/cm<sup>2</sup> for 24 hours in all parallel-plate flow chambers at 5% CO<sub>2</sub> and 37 °C.

## Animals

All animal experimentation was performed under the Institutional Animal Care and Use Committee-approved protocol #201303748.

## Mouse Intracranial Aneurysm Model

Murine intracranial aneurysms were created in female 8-12 week-old C57BL/6 mice (Charles River Laboratories, Wilmington, MA) using a method described previously.<sup>10</sup> For the antibody blockade, 100 µg/mL anti-CXCL1 antibody (MAB453, R&D Systems) or 100 µg/mL IgG2A control antibody were injected retro-orbitally every two days.

## Human Aneurysm and Superficial Temporal Artery Specimens

Collection of human cerebral aneurysm and superficial temporal artery specimens was performed under the IRB-approved protocols #448-2007 and #201400190. Patients gave written informed IRB research consent

## Statistical Analysis

Statistical analyses were performed by a biostatistician (DWN) and are described in detail in the online data supplement.

## Results

### Bifurcation and Bifurcation Aneurysm Parallel-Plate Flow Chamber Models Simulate Wall Shear Stress Patterns Found in Bifurcations and Cerebral Aneurysms

CFD studies of human and rabbit aneurysms have demonstrated that the average WSS within the aneurysm dome is lower than in the parent vessel.<sup>3-5, 8, 11</sup> We performed CFD analysis using Ansys FLUENT to obtain velocity magnitude, WSS, and WSSG maps of the flow field in the designed flow chambers (Fig 1A-C). The time-averaged WSS for the bifurcation flow chamber in the regions of interest where cells would be imaged were: 8.6 dyne/cm<sup>2</sup> in the proximal straight segment (PSS), 5.2 dyne/cm<sup>2</sup> at the bifurcation (B), and 4.3 dyne/cm<sup>2</sup> in the branching limbs (BL). For the bifurcation aneurysm flow chamber, WSS was 8.6 dyne/cm<sup>2</sup> in the proximal straight segment (PSS), 4.7 dyne/cm<sup>2</sup> at the bifurcation (B), 4.2 dyne/cm<sup>2</sup> in the branching limbs (BL), and 0.8 dyne/cm<sup>2</sup> within the aneurysm sac (AS).

### Low Hemodynamic Shear Stress and Shear Stress Gradients Upregulate Endothelial Expression of Inflammatory Mediators

We compared the inflammatory conditions across the three different flow chamber models (straight artery, bifurcation aneurysm, and arterial bifurcation, n=3 each) by using cytokine arrays. Multiple markers were upregulated in the bifurcation and bifurcation aneurysm flow models compared to the straight artery. IL-8 was the most differentially expressed cytokine (Fig 2A).

### Low Hemodynamic Shear Stress and Shear Stress Gradients at the Aneurysm Sac Microenvironment Upregulates IL-8 Expression

ELISA analysis of perfusate demonstrates that IL-8 secretion was significantly different across the three flow models ( $p=0.0238$ ). Significantly more IL-8 was secreted in the bifurcation aneurysm model (269.5 pg/mL,  $n=5$ ) than the bifurcation (146.8 pg/mL,  $n=5$ ,  $p=0.0395$ ) or straight model (147.5 pg/mL,  $n=5$ ,  $p=0.0409$ ) (Fig 2B). The difference between the bifurcation and straight models was not significant ( $p=0.9998$ ).

We investigated IL-8 expression by relative fluorescence-immunocytochemistry (RF-ICC) at different microenvironment sites *within* the bifurcation and the bifurcation aneurysm flow models to determine which microenvironment locales exposed to shear stress gradients are prone to inflammation. Within the bifurcation flow model, IL-8 expression was not significantly different among the bifurcation, the proximal straight segment (1.12 vs 1.00 RFU,  $p=0.55$ ), or the branching limb (1.12 vs 1.08,  $p=0.195$ ) microenvironments ( $n=24$  for each group,  $p=0.65$ ) (Figure 2C). The effect of microenvironment location on IL-8 protein expression in the bifurcation aneurysm model, however, was highly significant ( $n=24$  for each group,  $p<0.0001$ ) (Fig 2D). IL-8 protein expression in the aneurysm sac was estimated to be 33% higher than at the proximal straight segment (1.28 vs 1.00 RFU,  $p<0.0001$ ), 15% higher than at the branching limbs (1.28 vs 1.13 RFU,  $p=0.001$ ) and not significantly different than at the bifurcation (1.28 vs 1.13 RFU,  $p=0.144$ ). IL-8 expression at the proximal straight segment was estimated to be 26% lower than at the bifurcation (1.00 vs 1.12,  $p<0.001$ ) and 18% lower than at the branching limbs (1.00 vs 1.12 RFU,  $p<0.001$ ). IL-8 was 8% higher at the bifurcation than at the branching limbs (1.13 vs 1.12 RFU,  $p=0.009$ ). Representative IL-8 immunohistochemistry is shown for the bifurcation aneurysm chamber (Figure S3A).

### Low Hemodynamic Shear Stress and Shear Stress Gradients at the Bifurcation and Aneurysm Sac Microenvironments Upregulate CXCL1 Expression

CXCL1 is the closest functional murine homologue of IL-8. Since CXCL1 was not present on the original cytokine array panel (Fig 2A), we performed a CXCL1 ELISA on the perfusate from the same experimental samples. ELISA of 20x concentrated perfusing medium from the three different flow models demonstrates that CXCL1 secretion is significantly different across the three flow models ( $p<0.001$ ). Significantly more CXCL1 was secreted by ECs in the bifurcation flow model (34.3 pg/mL,  $n=7$ ) and bifurcation aneurysm flow model (64.8 pg/ml,  $n=7$ ) than in the straight flow model (14.4 pg/mL,  $n=9$ ,  $p=0.003$ ). The difference between CXCL1 expression in the bifurcation and bifurcation aneurysm flow models was not significant ( $p=0.477$ ) (Fig 2E).

CXCL1 protein expression at the three microenvironments *within* the bifurcation flow model was highly significant ( $n=24$  for each group,  $p<0.0001$  by mixed effects linear model) (Figure 2F). CXCL1 expression at the bifurcation was estimated to be 16% higher than at the proximal straight segment (1.16 vs 1.00 RFU,  $p<0.001$ ), and 7% higher than at the branching limbs (1.16 vs 1.08,  $p=0.039$ ). CXCL1 expression at the proximal straight segment was estimated to be 8% lower than at the branching limbs (1.00 vs 1.08 RFU,  $p=0.001$ ).

CXCL1 protein expression at the different microenvironments *within* the bifurcation aneurysm flow model was also highly significant (n=24 for each group, p<0.0001 by mixed effects linear model) (Figure 2G). CXCL1 expression at the aneurysm sac was estimated to be 29% higher than at the proximal straight segment (1.44 vs 1.00 RFU, p<0.001), 16% higher than at the bifurcation (1.44 vs 1.23 RFU, p<0.001) and 10% higher than at the branching limbs (1.44 vs 1.25 RFU, p=0.002). CXCL1 expression at the proximal straight segment was estimated to be 14% lower than at the bifurcation (1.00 vs 1.23 RFU, p<0.001) and 19% lower than at the branching limbs (1.00 vs 1.25 RFU, p<0.001). No difference was found in CXCL1 expression between the bifurcation and the limbs (p=0.224). These data confirm that the aneurysm sac microenvironment is the primary contributor of increased CXCL1. Representative CXCL1 immunohistochemistry is shown for the bifurcation aneurysm chamber (Figure S3B).

### ELR+ CXC Chemokines are Expressed in Human and Murine Aneurysms

The *in vitro* data obtained from our novel model is supported by our *in vivo* studies. Human aneurysm specimens tested positive for IL-8 and CXCL1 (n=5/5), whereas control superficial temporal arteries (STAs) did not (n=0/3) (Figure 3A and 3B).

Our mouse aneurysm model serves as a tool to further investigate this process. We analyzed the expression of ELR+ CXC chemokines, CXCL-1, -2, and -5-6/LIX in mouse 2-week aneurysms (Fig S4A and B). Reliable antibodies against CXCL3 are not available for use in mice. ELR+ CXC chemokines attract neutrophils and thus act as functional homologues of IL-8 in the mouse species.<sup>12</sup> CXCL1 was expressed in the intima and the media of 2-week (5/5) aneurysms and aneurysmal vessels (Fig S4B), whereas CXCL2 and CXCL5-6/LIX were not detected (0/5 for both). Furthermore, CXCL1 was expressed in 3-day and 1-week aneurysmal tissues but not in control arteries from sham animals (Fig 3C). ECs were visualized with MECA-32.

### CXCL1 Blockade Reduces Murine Intracranial Aneurysm Formation by Preventing Inflammatory Cell Infiltration

Mice treated with anti-CXCL1 antibody every 48 hrs (Fig 4A) developed significantly fewer saccular aneurysms than IgG-treated control mice at two weeks after aneurysm induction (13.3% vs 66.7%, p=0.0078, n=15 each) (Fig 4B and C). The majority of aneurysms were localized to arterial branch-points (Fig S5). The decrease in aneurysm formation in the anti-CXCL1 group was not attributable to changes in systemic systolic and diastolic blood pressure (Fig S6).

As expected, neutrophil infiltration in the anti-CXCL1-treated mice was significantly decreased at 2-weeks when compared with IgG control-treated mice (435 vs 2410 cells/mm<sup>2</sup>, n=15 for both, p=0.043) (Fig 5A and B). Macrophage infiltration in the anti-CXCL1-treated mice was not significantly different at 2-weeks when compared with IgG control-treated mice (7163 vs 9496 cells/mm<sup>2</sup>, n= 15 for both, p=0.056) (Fig 5C and D). In addition to endothelial and mural cells, infiltrating neutrophils were found to be positive for CXCR2, a receptor for CXCL1.

## Neutrophils and Macrophages Are Present in Human Aneurysms

All human aneurysm specimens analyzed were found to be positive for neutrophils and macrophages (n=5/5), while control STAs were negative (n=0/3) (Fig 5E).

## Discussion

Multiple studies have suggested a critical role for hemodynamics and inflammation in cerebral aneurysm formation<sup>3, 4, 6, 8, 11</sup> yet current tools to study this link are limited. We present a novel, idealized flow model based on PPFC geometry<sup>13</sup> and validated by computational fluid dynamics (Fig 1) that replicates WSS patterns typically seen at bifurcations and aneurysms. The advantages of this *in vitro* model over animal models are many: it is easy to use, low-cost, and produces results quickly. These characteristics make it ideal for initial high throughput screening to identify putative hemodynamic-induced inflammatory mediators that can then be validated *in vivo*.

There are limitations to this *in vitro* approach because radial stretch and 3-D matrices cannot be easily studied. The flow models represent idealized approximations of the hemodynamic shear stress patterns in bifurcations and bifurcation aneurysms<sup>3</sup> and lack an impingement zone near the flow divider.<sup>14</sup> Our goal was to study shear-stress cytokines released only by ECs and avoid interactions with vascular smooth muscle cells<sup>15</sup>; therefore, the model lacks the multi-cell layer characteristic of blood vessels. Despite these limitations, we were able to validate this powerful yet simple tool by identifying a novel role for IL-8 and CXCL1 in cerebral aneurysm formation (Fig 2).

The role of neutrophil-attracting ELR+ CXC chemokines, IL-8 and CXCL1<sup>12</sup>, has not been studied in cerebral aneurysm formation. Within the CXC family, the chemokines with an ELR+ (Glu-Leu-Arg) motif attract neutrophils.<sup>16, 17</sup> While, mice do not express IL-8,<sup>17</sup> CXCL1 has been described as a functional murine homologue of human IL-8.<sup>12</sup> CXCL1 shares more than 60% of amino acid sequence with IL-8 and activates the same receptor, CXCR2.<sup>18, 19</sup> Murine CXCL1 functions in inflammation, neutrophil chemotaxis, angiogenesis, and response to Prostaglandin E2 (PGE2) similar to human IL-8.<sup>12, 20-25</sup>

A low shear stress micro-environment is present within the aneurysm dome as soon as it forms.<sup>4, 8, 11</sup> Within the aneurysm dome the average WSS is lower than in the parent artery.<sup>3-5</sup> Recently, aneurysm growth has been reported to occur in regions of low WSS of the aneurysm dome.<sup>8, 11</sup> Low level shear stress can induce expression of ELR+CXC chemokines, primarily IL-8 and CXCL1 in the endothelium<sup>21</sup>, which upregulate ICAM, VCAM-1 and selectins.<sup>13</sup> Low or oscillatory shear stress in arterial bifurcations, stenosed or atherosclerotic vessels results in pro-inflammatory phenotype<sup>26</sup> through upregulation of NF- $\kappa$ B and IL-8 via MAPK.<sup>21</sup> Aoki et al found that hemodynamic shear stress activates the pro-inflammatory pathway NF- $\kappa$ B via PGE2 in cerebral aneurysms.<sup>6</sup> Activated platelets can release CXCL7, providing additional stimulus for neutrophil chemoattraction.<sup>27</sup> Conversely, neutrophils can bind to damaged EC wall and initiate thrombus formation.<sup>28</sup> In this work, we focused on cytokine profiling and neutrophil recruitment.

The bifurcation and aneurysm sac flow model microenvironments exposed to either low average hemodynamic shear stress or shear stress gradients were characterized by higher expression of CXCL1, and IL-8 and CXCL1, respectively (Fig 2). Elevated IL-8 in the blood of cerebral aneurysm patients has been reported<sup>29</sup> and CXCL1, the proposed murine functional homologue of human IL-8,<sup>17</sup> was the primary CXC chemokine expressed in murine aneurysms at 2 weeks after aneurysm induction (Fig S4). CXCL1 was also expressed at 3-days and 1-week (Fig 3C).

Murine cerebral aneurysm formation (Fig 4) and neutrophil infiltration (Fig 5) were significantly decreased following CXCL1 antibody blockade. Formation of aneurysms in our murine model is dependent upon the combination of hypertensive and angiotoxic insults.<sup>10</sup> Hypertension is created via high salt diet, carotid and renal artery ligations, and Angiotensin II-releasing pump. Angiotoxic effects of BAPN with damage to the elastin layer by elastase injection provide the final stimulus for aneurysm formation. Differences in aneurysm formation between the anti-CXCL1 and IgG groups could not be attributed to changes in systemic blood pressure (Fig S6). Rather, blockade of CXCL1 likely reduces aneurysm formation and neutrophil infiltration by discouraging cell-cell interactions between the endothelium and immune cells. By upregulating VCAM-1 on the cell surface, CXCL1 effectively arrests monocytes.<sup>30</sup> VCAM-1 facilitates monocyte<sup>30</sup> and neutrophil binding<sup>17</sup> to the activated endothelium. Indeed, VCAM-1 was increased in the endothelium in the aneurysm sac of the bifurcation aneurysm flow chamber model when compared to other microenvironments, and in the aneurysms of IgG-treated mice (Fig S7 and S8).

## Perspectives

Using our novel model, we demonstrate for the first time to our knowledge that shear stress-mediated endothelial inflammation and CXCL1-dependent neutrophil recruitment are important factors in cerebral aneurysm formation. This is significant, as neutrophils have been largely neglected in study of cerebral aneurysms. We speculate that blocking shear stress induced-CXCL1 could be used to prevent new cerebral aneurysm formation and/or growth of established lesions. The novel methods and findings presented here will promote further insights into link between hemodynamics and inflammation in cerebral aneurysm development.

## Supplementary Material

Refer to Web version on PubMed Central for supplementary material.

## Acknowledgments

We would like to thank Dan Neal, MS for performing the detailed statistical analysis, Joseph Uzarski, PhD for endothelial cell isolation and professional advice, and Matheus Schneider for blood pressure measurements.

Funding Sources: This work was supported by a grant from the Brain Aneurysm Foundation to KWN and NIH grant K08 NS067058-01 to BLH.

## References

1. Wiebers DO, Whisnant JP, Huston J 3rd, Meissner I, Brown RD Jr, Piepgras DG, Forbes GS, Thielen K, Nichols D, O'Fallon WM, Peacock J, Jaeger L, Kassell NF, Kongable-Beckman GL, Torner JC, International Study of Unruptured Intracranial Aneurysms I. Unruptured intracranial aneurysms: Natural history, clinical outcome, and risks of surgical and endovascular treatment. *Lancet*. 2003; 362:103–110. [PubMed: 12867109]
2. Alfano JM, Kolega J, Natarajan SK, Xiang J, Paluch RA, Levy EI, Siddiqui AH, Meng H. Intracranial aneurysms occur more frequently at bifurcation sites that typically experience higher hemodynamic stresses. *Neurosurgery*. 2013; 73:497–505. [PubMed: 23756745]
3. Sforza DM, Putman CM, Cebal JR. Hemodynamics of cerebral aneurysms. *Annual review of fluid mechanics*. 2009; 41:91–107.
4. Shojima M, Oshima M, Takagi K, Torii R, Hayakawa M, Katada K, Morita A, Kirino T. Magnitude and role of wall shear stress on cerebral aneurysm: Computational fluid dynamic study of 20 middle cerebral artery aneurysms. *Stroke; a journal of cerebral circulation*. 2004; 35:2500–2505.
5. Valencia A, Morales H, Rivera R, Bravo E, Galvez M. Blood flow dynamics in patient-specific cerebral aneurysm models: The relationship between wall shear stress and aneurysm area index. *Medical engineering & physics*. 2008; 30:329–340. [PubMed: 17556005]
6. Aoki T, Nishimura M, Matsuoka T, Yamamoto K, Furuyashiki T, Kataoka H, Kitaoka S, Ishibashi R, Ishibazawa A, Miyamoto S, Morishita R, Ando J, Hashimoto N, Nozaki K, Narumiya S. Pge(2) - ep(2) signalling in endothelium is activated by haemodynamic stress and induces cerebral aneurysm through an amplifying loop via nf-kappab. *British journal of pharmacology*. 2011; 163:1237–1249. [PubMed: 21426319]
7. Uzarski JS, Scott EW, McFetridge PS. Adaptation of endothelial cells to physiologically-modeled, variable shear stress. *PloS one*. 2013; 8:e57004. [PubMed: 23457646]
8. Tanoue T, Tateshima S, Villablanca JP, Vinuela F, Tanishita K. Wall shear stress distribution inside growing cerebral aneurysm. *AJNR American journal of neuroradiology*. 2011; 32:1732–1737. [PubMed: 21984256]
9. Murray KD. Dimensions of the circle of willis and dynamic studies using electrical analogy. *Journal of neurosurgery*. 1964; 21:26–34. [PubMed: 14110356]
10. Hosaka K, Downes DP, Nowicki KW, Hoh BL. Modified murine intracranial aneurysm model: Aneurysm formation and rupture by elastase and hypertension. *Journal of neurointerventional surgery*. 2014; 6:474–479. published online ahead of print, August 13, 2013. <http://jn.is.bmj.com/content/6/6/474.long>. 10.1136/neurintsurg-2013-010788 [PubMed: 23943816]
11. Kadirvel R, Ding YH, Dai D, Zakaria H, Robertson AM, Danielson MA, Lewis DA, Cloft HJ, Kallmes DF. The influence of hemodynamic forces on biomarkers in the walls of elastase-induced aneurysms in rabbits. *Neuroradiology*. 2007; 49:1041–1053. [PubMed: 17882410]
12. Hol J, Wilhelmssen L, Haraldsen G. The murine il-8 homologues kc, mip-2, and lix are found in endothelial cytoplasmic granules but not in weibel-palade bodies. *Journal of leukocyte biology*. 2010; 87:501–508. [PubMed: 20007247]
13. Lawrence MB, McIntire LV, Eskin SG. Effect of flow on polymorphonuclear leukocyte/ endothelial cell adhesion. *Blood*. 1987; 70:1284–1290. [PubMed: 3663936]
14. Szymanski MP, Metaxa E, Meng H, Kolega J. Endothelial cell layer subjected to impinging flow mimicking the apex of an arterial bifurcation. *Annals of biomedical engineering*. 2008; 36:1681–1689. [PubMed: 18654851]
15. Wallace CS, Truskey GA. Direct-contact co-culture between smooth muscle and endothelial cells inhibits tnf-alpha-mediated endothelial cell activation. *American journal of physiology. Heart and circulatory physiology*. 2010; 299:H338–346. [PubMed: 20495148]
16. Bizzari C, Beccari AR, Bertini R, Cavicchia MR, Giorgini S, Allegretti M. Elr+ cxc chemokines and their receptors (cxc chemokine receptor 1 and cxc chemokine receptor 2) as new therapeutic targets. *Pharmacology & therapeutics*. 2006; 112:139–149. [PubMed: 16720046]
17. Kolaczowska E, Kubes P. Neutrophil recruitment and function in health and inflammation. *Nature reviews. Immunology*. 2013; 13:159–175.



18. Ohmori Y, Hamilton TA. A macrophage lps-inducible early gene encodes the murine homologue of ip-10. *Biochemical and biophysical research communications*. 1990; 168:1261–1267. [PubMed: 2189406]
19. Bozic CR, Gerard NP, von Uexkull-Guldenband C, Kolakowski LF Jr, Conklyn MJ, Breslow R, Showell HJ, Gerard C. The murine interleukin 8 type b receptor homologue and its ligands. Expression and biological characterization. *The Journal of biological chemistry*. 1994; 269:29355–29358. [PubMed: 7961909]
20. Bickel M. The role of interleukin-8 in inflammation and mechanisms of regulation. *Journal of periodontology*. 1993; 64:456–460. [PubMed: 8315568]
21. Shaik SS, Soltau TD, Chaturvedi G, Totapally B, Hagoood JS, Andrews WW, Athar M, Voitenok NN, Killingsworth CR, Patel RP, Fallon MB, Maheshwari A. Low intensity shear stress increases endothelial elr+ cxc chemokine production via a focal adhesion kinase-p38{beta} mapk-nf- $\kappa$ b pathway. *The Journal of biological chemistry*. 2009; 284:5945–5955. [PubMed: 19117939]
22. Smith WB, Gamble JR, Clark-Lewis I, Vadas MA. Interleukin-8 induces neutrophil transendothelial migration. *Immunology*. 1991; 72:65–72. [PubMed: 1997402]
23. Wang D, Wang H, Brown J, Daikoku T, Ning W, Shi Q, Richmond A, Strieter R, Dey SK, DuBois RN. Cxcl1 induced by prostaglandin e2 promotes angiogenesis in colorectal cancer. *The Journal of experimental medicine*. 2006; 203:941–951. [PubMed: 16567391]
24. Yu Y, Chadee K. Prostaglandin e2 stimulates il-8 gene expression in human colonic epithelial cells by a posttranscriptional mechanism. *Journal of immunology*. 1998; 161:3746–3752.
25. Yue TL, Wang X, Sung CP, Olson B, McKenna PJ, Gu JL, Feuerstein GZ. Interleukin-8. A mitogen and chemoattractant for vascular smooth muscle cells. *Circulation research*. 1994; 75:1–7. [PubMed: 8013067]
26. Chiu JJ, Chien S. Effects of disturbed flow on vascular endothelium: Pathophysiological basis and clinical perspectives. *Physiological reviews*. 2011; 91:327–387. [PubMed: 21248169]
27. Brandt E, Petersen F, Ludwig A, Ehlert JE, Bock L, Flad HD. The beta-thromboglobulins and platelet factor 4: Blood platelet-derived cxc chemokines with divergent roles in early neutrophil regulation. *Journal of leukocyte biology*. 2000; 67:471–478. [PubMed: 10770278]
28. Darbousset R, Thomas GM, Mezouar S, Frere C, Bonier R, Mackman N, Renne T, Dignat-George F, Dubois C, Panicot-Dubois L. Tissue factor-positive neutrophils bind to injured endothelial wall and initiate thrombus formation. *Blood*. 2012; 120:2133–2143. [PubMed: 22837532]
29. Chalouhi N, Points L, Pierce GL, Ballas Z, Jabbour P, Hasan D. Localized increase of chemokines in the lumen of human cerebral aneurysms. *Stroke; a journal of cerebral circulation*. 2013; 44:2594–2597.
30. Huo Y, Weber C, Forlow SB, Sperandio M, Thatte J, Mack M, Jung S, Littman DR, Ley K. The chemokine kc, but not monocyte chemoattractant protein-1, triggers monocyte arrest on early atherosclerotic endothelium. *The Journal of clinical investigation*. 2001; 108:1307–1314. [PubMed: 11696575]

## Novelty and Significance

### What Is New?

In vitro approach can be used to identify hemodynamic-induced inflammatory mediators of cerebral aneurysm formation. Hemodynamic shear stress leads to increased endothelial secretion of IL-8 and CXCL1 in cerebral aneurysms. CXCL1 is the primary ELR+CXC chemokine expressed in murine cerebral aneurysms. Anti-CXCL1 blockade significantly decreases murine cerebral aneurysm formation through decreased neutrophil recruitment.

### What Is Relevant?

Inflammation is a hallmark feature of cerebral aneurysms, however, early molecular events in aneurysm formation are still not fully understood. This study addressed the link between hemodynamic shear stress and early inflammatory mediators and through a combination of in silico, in vitro, and in vivo approach demonstrates a critical role for shear stress-induced CXCL1-dependent neutrophil recruitment in cerebral aneurysm formation.

### Summary

Cerebral aneurysm formation is an inflammatory mediated process driven by abnormal hemodynamic shear stress. Our study offers a new in vitro model for study of cerebral aneurysm formation. Our data suggest that CXCL1-dependent neutrophil infiltration may be a target for therapeutic intervention for cerebral aneurysms.

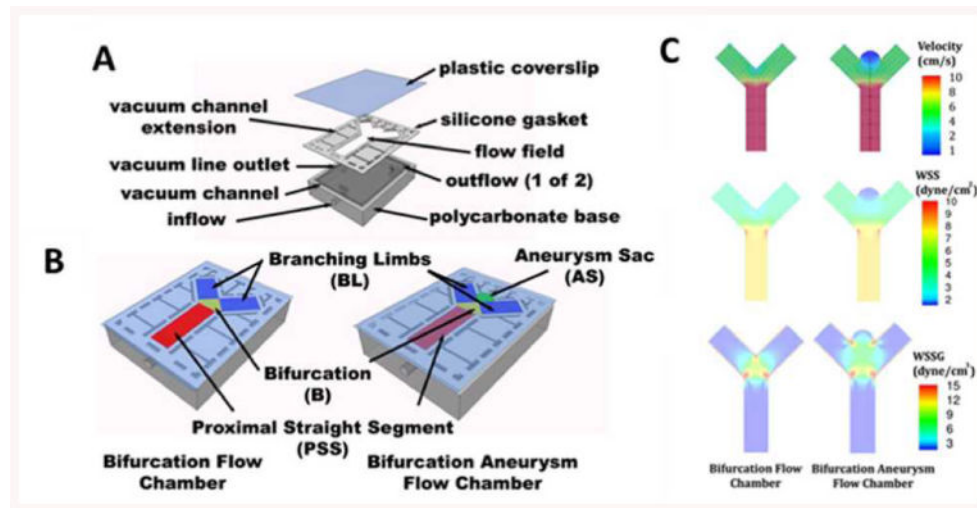


**Figure 1.** Bifurcation and bifurcation aneurysm flow chamber design and computational fluid dynamics.

A) 3-D model showing plastic coverslip, silicone gasket with the flow field, and polycarbonate bioreactor cell. B) Complete, sealed chambers with color-coded maps showing components of the flow field. C) CFD showing velocity, wall shear stress (WSS), and wall shear stress gradient (WSSG) within the designed flow chambers.

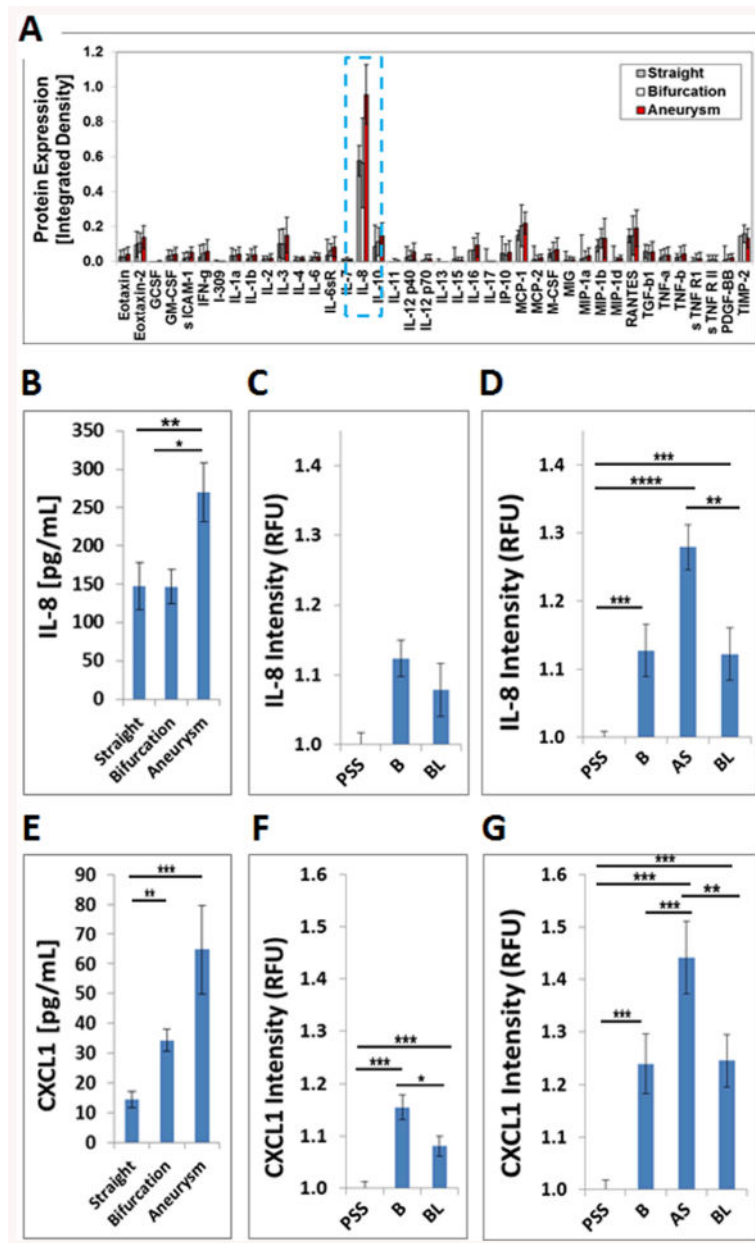


**Figure 2.** ELR+CXC chemokines IL-8 and CXCL1 are the most abundantly expressed cytokines in the bifurcation aneurysm flow chamber. A) Chemokine profiles of HUVECs exposed to pulsatile flow in different flow chambers. Out of 40 inflammatory cytokines analyzed, B) IL-8 was the most abundant differentially expressed cytokine in the aneurysm flow chamber, which was confirmed by IL-8 ELISA ( $p=0.0238$ ). C) IL-8 expression in the bifurcation flow chamber is not significantly different ( $p=0.065$ ). D) HUVECs express more IL-8 in the aneurysm and bifurcation regions of the bifurcation aneurysm flow chamber ( $p<0.0001$ ). E) HUVECs express more CXCL1 in the bifurcation and bifurcation aneurysm models than in the straight flow model ( $p=0.0076$ ). F) HUVECs express more CXCL1 in the bifurcation region of the bifurcation flow chamber ( $p<0.0001$ ). G) HUVECs express more CXCL1 in

the aneurysm sac of the bifurcation aneurysm flow chamber ( $p < 0.0001$ ). (\*  $p < 0.05$ , \*\*  $p < 0.01$ , \*\*\*  $p < 0.001$ , \*\*\*\*  $p < 0.0001$ ). Data are presented as mean  $\pm$  s.e.m.

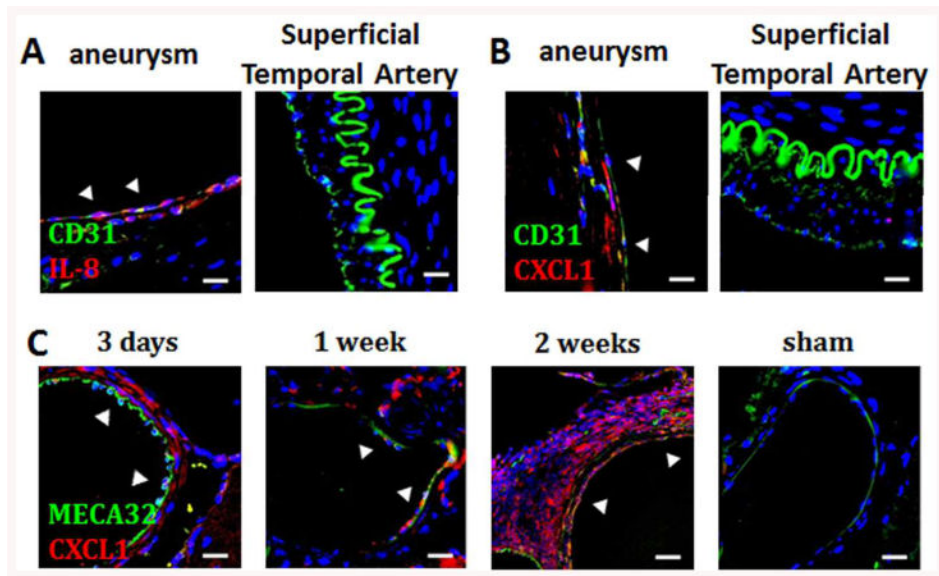


**Figure 3.** ELR+CXC chemokine expression in human and murine aneurysms. A) Endothelial cells in human aneurysm tissues are positive for IL-8 (arrows) whereas endothelial cells in control superficial temporal arteries (STA) are negative (*Blue*: DAPI, *Green*: CD31, *Red*: IL-8, scalebar=10 μm). B) Endothelial cells in human aneurysms are positive for CXCL1 (arrows) whereas endothelial cells in control STAs are negative. (*Blue*: DAPI, *Green*: CD31, *Red*: CXCL1, scalebar=10 μm). C) CXCL1 expression in mouse aneurysmal vessels and aneurysm specimens is present in the media at 3 days, 1- and 2-weeks, while arteries from sham mice are negative. (*Blue*: DAPI, *Green*: CD31, *Red*: CXCL1, scalebar=10 μm).

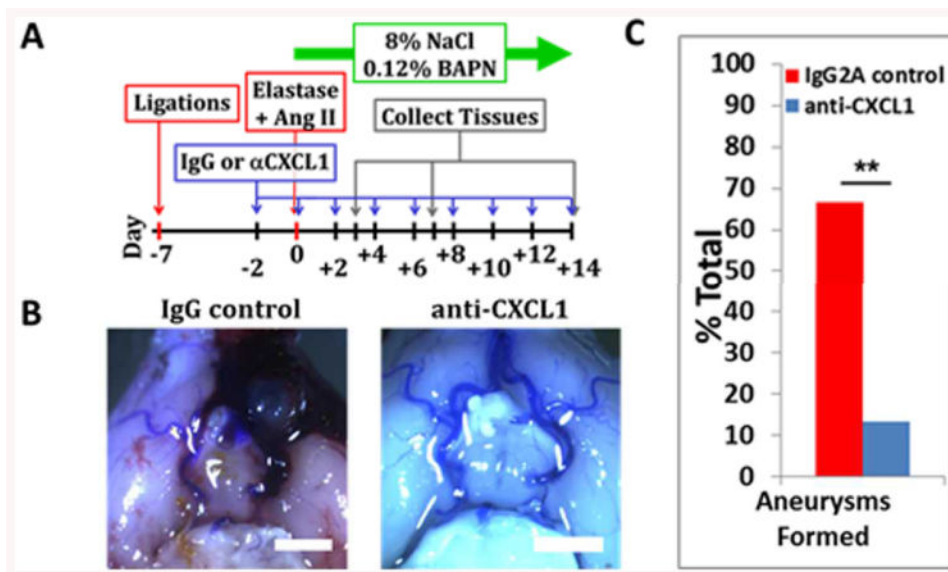


**Figure 4.** CXCL1 blockade prevents mouse intracranial aneurysm formation  
 A) Experimental scheme. B) Representative pictures of Circle of Willis from IgG- and anti-CXCL1-treated mice (scalebar=2 mm). C) Mice treated with CXCL1-neutralizing antibody over two weeks develop significantly less aneurysms than IgG2A treated mice ( $p=0.0078$ ). Data are presented as mean $\pm$ s.e.m.

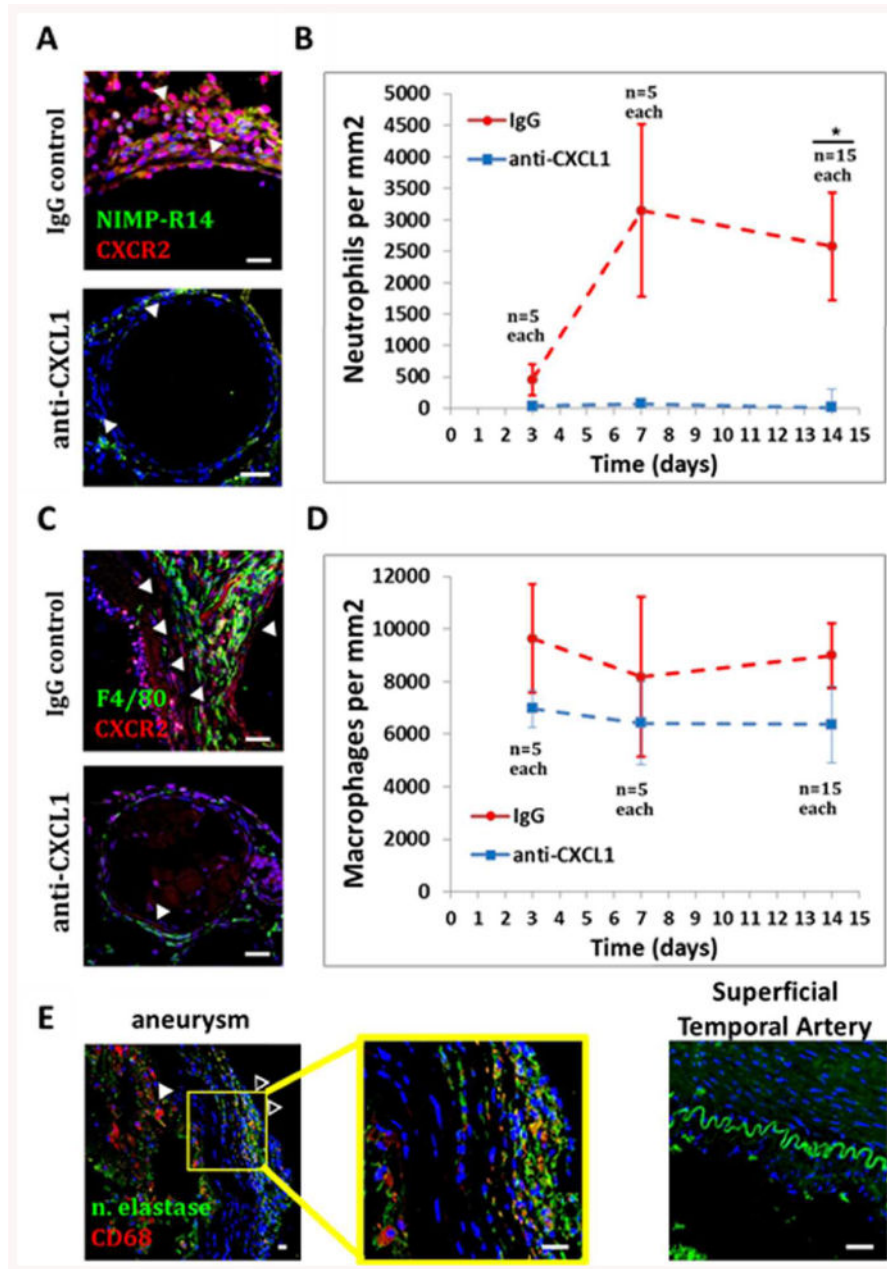


**Figure 5.** Effects of CXCL1 blockade on inflammatory cell infiltration. CXCL1 blockade over two weeks results in A and B) significantly less neutrophil infiltration ( $p=0.043$ ) (Blue: DAPI, Green: NIMP-R14, Red: CXCR2, scalebar=10  $\mu$ m). C and D) No significant differences in macrophage infiltration were found ( $p=0.056$ ) (Blue: DAPI, Green: F4/80, Red: CXCR2, scalebar=10  $\mu$ m). E) Human aneurysm specimens are positive for infiltrating neutrophils (open arrows) and macrophages (full arrows) while control STAs are negative (Blue: DAPI, Green: neutrophil elastase, Red: CD68, scalebar=10  $\mu$ m). Data are presented as mean $\pm$ s.e.m.